# Dynamics of an Ising Chain under Local Excitation: A Scanning Tunneling Microscopy Study of Si(100) Dimer Rows at 5 K

Y. Pennec,[1] M. Horn von Hoegen,[2] Xiaobin Zhu,[1] D. C. Fortin,[1] and M. R. Freeman[1,3]
[1]*Department of Physics, University of Alberta, Edmonton, Canada T6G 2J1*
[2]*Department of Physics, University of Duisburg-Essen, 45117 Essen, Germany*
[3]*National Institute for Nanotechnology, Edmonton, Canada T6G 2V4*
(Received 12 August 2005; published 20 January 2006)

An extension of the classical Ising model to a situation including a source of spin-flip excitations localized on the scale of individual spins is considered. The scenario is realized by scanning tunneling microscopy of the Si(100) surface at low temperatures. Remarkable details, corresponding to the passage of phasons through the tunnel junction, are detected by the STM within the short span between two atoms comprising an individual Si dimer.

DOI: 10.1103/PhysRevLett.96.026102 PACS numbers: 68.35.Ja, 68.37.Ef, 75.10.Hk, 85.90.+h

Despite intensive study over the past several decades, scientific interest in the Si(100) surface continues unabated [1–3], and complements the immense importance of this surface to semiconductor device technology [4], molecular electronics [5], and novel computation schemes [6]. The building block of this surface is a ''buckled'' dimer, a bistable mechanical equivalent of a magnetic Ising spin. The temperature-dependent phase reconstruction of the surface is well described by an Ising model with a nearest neighbor ''antiferromagnetic'' interaction between the dimers [7]. This strongly anisotropic interaction leads to the formation of rows of dimers of alternating tilt, a model system for the antiferromagnetic classical Ising chain [8].

A key recent discovery has been the ability to induce reconstructions of this surface via scanning tunneling microscopy at low temperatures [9,10]. This observation plays into earlier suggestions to exploit the surface for a microscopic implementation of dimer logic and memories [6], based upon the two-state nature of the system and the potential to flip the dimers directly with an STM. Viewed as electromechanical components, these dimers are essentially at the ultimately smallest conceivable size. In this Letter we report a detailed investigation of an alternative mechanism for dimer flipping suggested by the Ising model. A phenomenological model is elaborated through kinetic Monte Carlo simulations which capture the essential features of the experimental observations. When the tip is tunneling, at high enough bias, into a row containing a phase defect in the dimer alignment [a zero-dimensional domain wall or ''phason'' [11]], this phason undergoes a biased random walk, with a tendency for attraction towards the tip. The dimer under the tunneling tip is flipped each time the phason transits through this junction. The study reveals general characteristics of a classical Ising chain subject to a localized excitation.

The measurements were performed using an ultrahigh vacuum ($2 \times 10^{-11}$ mbar), low temperature (5 K), and high stability beetle-type scanning tunneling microscope [12]. A heavily As-doped $n$-type Si(100) sample (0.003–0.004 $\Omega$ cm at room temperature, from Virginia Semiconductor) was prepared through heating and flash annealing to achieve a low defect-density surface [13]. An electrochemically etched tungsten tip was cleaned via electron bombardment. The tip could be ''resharpened'' *in situ* through tip forming on an adjacent Au specimen on the sample holder [14]. Figure 1 summarizes the phenomenology of the Si(100) surface as found in empty-state

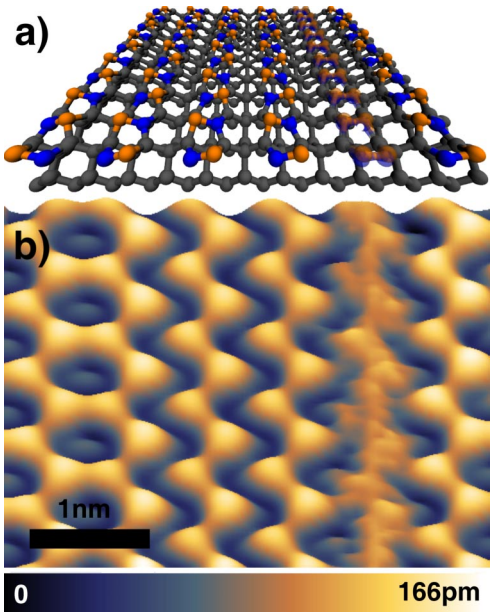


FIG. 1 (color online). The Si(100) surface in (a) ball-and-stick representation and (b) an empty-state STM micrograph (sample bias +1.35 V/tunnel current 1nA) at $T = 5$ K. Both the top and bottom dimer atoms appear in the two $c(4 \times 2)$ reconstructed rows on the left-hand side. The one-dimensional nature of the chains is highlighted by the chevron pattern of the $p(2 \times 2)$ reconstruction. The noisy section arises from switching of the dimer buckling angle when the tip is tunneling into that row.

 

imaging by STM. Figure 1(b) shows a typical topograph ($T = 5$ K, sample bias $+1.35$ V, current 1 nA) where the equivalent atomic positions [15] are easily recognized on the ball-and-stick model of Fig. 1(a). The left part of the image is $c(4 \times 2)$ reconstructed (appearing with quasi-sixfold symmetry), and a zigzag or chevron pattern appears when the local reconstruction is $p(2 \times 2)$. A single row appears noisy. At higher sample temperatures this flickering noise usually has been interpreted as resulting from the local switching of the tilt of a single dimer under the tip due to thermal fluctuations. The thermal activation of dimer flipping has been studied by Hata *et al.* at $T = 80$ K [16] and the energy barrier estimated to be on the order of 100 meV. At $T = 5$ K, the thermal energy is so low in relation to the barrier height that this mechanism is inoperative. However, from earlier STM studies of Si(100) at low temperatures, it is well known that tunneling conditions affect the appearance of the surface. It has been recently shown that manipulation between the $c(4 \times 2)$, $p(2 \times 2)$, and $p(2 \times 1)$ reconstructions may be achieved by bias voltage control [9]. The physics of this phenomenon remains debated, but three main processes have to be taken into account: inelastic scattering, tip-sample interaction, and surface charging [17–22]. For the present investigation we focus on tunneling conditions where, based upon the earlier work, one expects the surface to present both $c(4 \times 2)$ and $p(2 \times 2)$ states, and rows of unstable dimers. A simple question raised by the experiment of Fig. 1(b) is: why do only particular rows flicker during the acquisition of the image?

In order to elucidate the flickering dynamics, Fig. 2 presents high spatial resolution measurements of the noise properties across a single flickering dimer row. In this measurement the feedback time constant (2 sec) is set to be longer than the slowest characteristic flickering time (0.1 sec), and the scanning time constant (5 sec per pixel) is slower still. A 1 s current record is acquired at a 10 kHz sampling rate at each position as the tip position is incremented in 25 pm steps. Three current traces are presented in Fig. 2(a). The top trace, acquired over one of the quiet rows, is presented for reference. The middle trace is from the center of the flickering row, where the tunneling current should be independent of the tilt of a single flip-flopping dimer. Surprisingly, the current trace at this location is found to exhibit sharp downward spikes. The bottom trace, collected above the ''left'' atom of the dimer, is reminiscent of two-state telegraph noise, but with additional levels likely also present. For further visualization of the overall switching behavior, the time records have been projected onto individual histograms and assembled into a two-dimensional plot in Fig. 2(b). This rendering illustrates, as a function of position, the relative probability of observing a particular tunneling conductance. The superimposed curves represent a quantitative derivation of the envelope predicted from a tip-sample distance model based on a

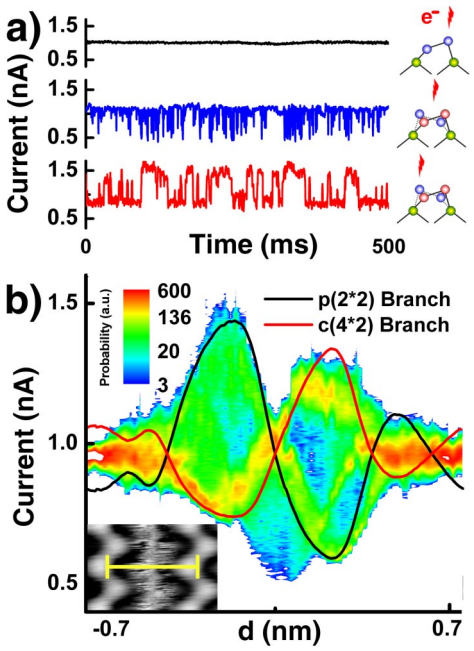


FIG. 2 (color online). (a) Traces of the current vs time (tip at constant height in each case), showing three behaviors: constant current over a quiet row (top), fast downward spikes in the current above the center position in a noisy row (middle), telegraph noise atop an atom position in a noisy row (bottom). (b) A histogram representation of the position-dependent current recordings shows the tunneling conductance splitting and crossing over in a characteristic ''figure eight'' pattern across the dimer. Two main levels forming the outer envelope are identified as the $c(4 \times 2)$ or $p(2 \times 2)$ local reconstruction of the row, through a simple tip-sample distance model. Superimposed upon this pattern is a U-shaped background of current levels with the signature characteristic that it plunges significantly below the central crossover of the figure eight. This feature arises from the passage of a phason under the tip. The inset shows an STM scan (1 nA/1.35 V) of the same area.

dimer switching back and forth between a pure $c(4 \times 2)$ and a pure $p(2 \times 2)$ local reconstruction. Qualitatively, the plots of Fig. 2(b) correspond mainly to a sideways ''figure eight'' shape, as one might expect to arise from simple seesaw motion of the dimer. More importantly, the plot reveals details not captured within that simple picture. ''Deeper'' (lower current) states appear near the middle of the dimer [blue trace in Fig. 2(a)], where the tunneling current should be approximately the same for both tilts of the dimer. These downward current spikes reflect the passage of a phason through the tunnel junction, as elaborated below. The measurement highlights the ability of the STM to resolve lateral information on the picometer scale [23,24].

Bias-dependent imaging of the surface is able to capture static phasons at low bias, and correlate these with flickering rows at higher bias. A stationary phason appears as a domain wall between local $c(4 \times 2)$ and $p(2 \times 2)$ configurations along a row. Repeated STM images of the same

area, taken in succession at two different bias voltages, are presented in Fig. 3. The left scan is acquired at a sample bias of 983 mV. In this case the tip-induced excitation is suppressed and we are able to observe clearly the occasional stationary phason, identifiable along some dimer rows as the transition between a $c(4 \times 2)$ and a $p(2 \times 2)$ local configuration. When the bias voltage is raised sufficiently to reactivate flickering and the same area is then rescanned (Fig. 3, right panel), it is found that the rows previously found to contain a phason have now become noisy. This lends additional support to the interpretation that the tunneling-induced dynamics are not due to the local flickering of an individual dimer under the tip, but to a random walk motion of a phason. Note that in the rescan, the flickering can already appear in a row at a significant distance from where the phason was seen statically, demonstrating that there is (on the atomic scale) a ''long-range'' action of the excitation by the tunneling probe [24].

It is natural to describe the results by an extension of the Ising viewpoint employed successfully in descriptions of the Si(100) surface. We use a kinetic Monte Carlo (KMC) approach, as has been applied to the thermally activated flickering of the surface [25]. The probability of flipping of any one of the spins in the chain is proportional to $r_n = r_o e^{\beta_n \Delta E_n}$, where $\beta_n$ is one over the *local* excitation energy in this case, and $\Delta E_n$ is the height of the barrier and depends on the neighbor configuration. The attempt frequency $r_o$ is taken to be 1 GHz, the range generally estimated for this system [16,17].

The inelastic scattering of hot electrons with Si(100) dimers has been discussed by Kawai [17]. At low temperatures the deexcitation rate of the dimer rocking mode vibrational state is low and tunneling of hot electrons via the STM tip will raise the dimer effective temperature. Moreover, two-photon photoemission spectroscopy measurements at 80 K show that an excited hot electron will remain in the surface and propagate along the chain [26]. The primary mechanism for the long-range action on the phason observed in these experiments is likely the excitation of dimer rocking vibrations along the thermalization path of the electron. In the modeling results below [27], the essential physical point is that switching a spin within a phason is energetically much easier than flipping a ''satisfied'' spin elsewhere in the chain.

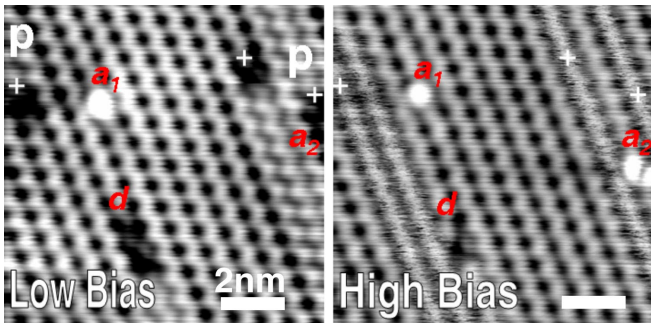


FIG. 3 (color online). Bias-dependent imaging of the neighborhood of flickering rows. Left panel: scan at $V = 983$ mV/$I = 89$ pA containing three phasons, labeled $P$, which appear deeper in the center than a normal dimer. In addition, there is another defect ($d$) [30] and two kinds of adsorbates ($a_1$ and $a_2$) within the imaged area. Right panel: scan at $V = 1296$ mV/$I = 89$ pA shows correlation between the flickering rows and the phason-containing rows found at lower bias.

Consider the results of the simulation for the different scenarios characteristic of the experiments. The three panels in Fig. 4(c) are to be compared with those in Fig. 2(a). A qualitative representation of the tunneling signal versus time is obtained from the model by translating the spin configuration at the tip location (current injection point) to an effective conductance, recognizing that this mapping depends upon whether the dimer under the tip is tilted left

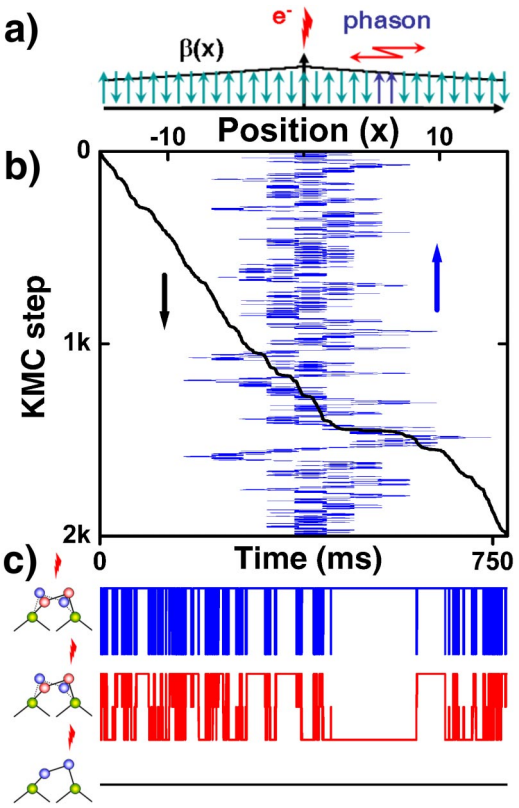


FIG. 4 (color online). (a) Schematic of the locally excited antiferromagnetic classical Ising chain containing a phason. The excitation rate $\beta$ is taken to decay exponentially away from the tip position, along the row. (b) Position of the phason ( gray trace, blue online) as the KMC algorithm iterates, and the translation of KMC step to time (black trace, bottom axis). (c) Flickering characteristics obtained from the model for three scenarios: top, tunneling into the central dimer position of a row containing a phason in the initial state; middle, tunneling into a position on top of a dimer atom, for a row containing a phason; bottom, tunneling into a row with perfect antiferromagnetic order.

or right, or is part of a phason. The two upper frames of Fig. 4(c) present the modeled time evolution of the tunneling signal for the mappings which assume that the tunneling point is at the middle of a dimer (top) and above a dimer atom (middle), when a phason is included in the initial state of the chain. The origin of the instability is shown by Fig. 4(b), where the position of the phason is represented versus the KMC step. The flipping of the spin under the tip is effected by a biased random walk motion of the phason. The random walk exhibits two generic features of the locally excited Ising chain. First the tip acts as an attractor for the phason, because it is always slightly more favorable to switch the spin of the phason that is nearer to the injection point. Second, the ''telegraph noise'' of the central spin contains bursts from fast motion just under the tip, interrupted on occasion by longer intervals when the phason is farther away from the tip. This effect is enhanced by the strong decrease of the phason velocity at increased distance from the tip where the excitation strength is reduced, and is revealed by the strong nonlinearity of the plot of time versus KMC step from the model [black trace in Fig. 4(b)]. Finally, the bottom trace in Fig. 4(c) results from a simulation where the initial state of the chain did not contain a phason. In this time frame, the switching rate for a stable spin is so low that the trace remains flat.

In conclusion, we have reported a study of the response of an Ising chain to a local excitation, implemented through measurements of STM-induced flickering of individual dimer rows on the Si(100) surface. A model of phason motion induced by inelastic scattering of hot electrons has been proposed, and explains the onset and termination of flickering of individual rows, the qualitative temporal characteristics of the flicker noise, and the appearance of unexpected spatial structure in the tunnel current measurements. Through the excitation of ''spin flips'' on a local scale in a mechanical analog, this system relates to the fascination of single spin phenomena [28] and allows a beginning study, on the scale of the individual spins, of collective effects arising in ordered few-spin systems. In prospective implementations of dimer logic schemes using Ising chains, it may be necessary to eliminate the propagation of phasons, for example, through the judicious placement of adsorbates. Alternatively, one might exploit dimer phasons themselves as the operative bits, in analogy with magnetic domain wall logic [29].

We gratefully acknowledge NSERC, iCORE, CIAR, CRC, CFI, ASRA, and DFG SFB616 (MHvH) for financial support. We thank Professor Frank Marsiglio for fruitful discussions, Tyler Luchko for assistance with VMD, and Professor Robert Wolkow for a critical reading of the manuscript.

[1] R. E. Schlier and H. E. Farnsworth, J. Chem. Phys. **30**, 917 (1959).
[2] R. A. Wolkow, Phys. Rev. Lett. **68**, 2636 (1992).
[3] S. Yoshida *et al.*, Phys. Rev. B **70**, 235411 (2004).
[4] S. Sze, *Physics of Semiconductor Devices* (Wiley, New York, 1981), 2nd ed.
[5] P. G. Piva *et al.*, Nature (London) **435**, 658 (2005).
[6] I. Appelbaum, J. D. Joannopoulos, and V. Narayanamurti, Phys. Rev. E **66**, 066612 (2002).
[7] J. Ihm *et al.*, Phys. Rev. Lett. **51**, 1872 (1983).
[8] E. Ising, dissertation, University of Hamburg, 1924.
[9] K. Sagisaka, D. Fujita, and G. Kido, Phys. Rev. Lett. **91**, 146103 (2003).
[10] K. Sagisaka and D. Fujita, Phys. Rev. B **71**, 245319 (2005).
[11] S. Yoshida *et al.*, Jpn. J. Appl. Phys. **41**, 5017 (2002).
[12] G. Meyer, Rev. Sci. Instrum. **67**, 2960 (1996); microscope from SPS Createc GmbH.
[13] K. Hata *et al.*, J. Vac. Sci. Technol. A **18**, 1933 (2000).
[14] M. Horn von Hoegen *et al.* (to be published).
[15] A. Ramstad, G. Brocks, and P. J. Kelly, Phys. Rev. B **51**, 14 504 (1995).
[16] K. Hata, Y. Sainoo, and H. Shigekawa, Phys. Rev. Lett. **86**, 3084 (2001).
[17] H. Kawai and O. Narikiyo, J. Phys. Soc. Jpn. **73**, 417 (2004).
[18] S. Yoshida *et al.*, Phys. Rev. B **70**, 235411 (2004).
[19] T. Shirasawa, S. Mizuno, and H. Tochihara, Phys. Rev. Lett. **94**, 195502 (2005).
[20] M. Dubois *et al.*, Phys. Rev. B **71**, 165322 (2005).
[21] G. P. Kochanski and J. E. Griffith, Surf. Sci. Lett. **249**, L293 (1991).
[22] F. H. Stillinger, Phys. Rev. B **46**, 9590 (1992).
[23] M. Lastapis *et al.*, Science **308**, 1000 (2005).
[24] See EPAPS Document No. E-PRLTAO-96-052604. An EPAPS document linked to the online version contains supplementary information concerning images of static phasons acquired after alternate applications of higher bias, and spectral analysis of the time series current measurements. This document can be reached via a direct link in the online article's HTML reference section or via the EPAPS homepage (http://www.aip.org/pubservs/epaps.html).
[25] A. Natori *et al.*, Appl. Surf. Sci. **212–213**, 705 (2003).
[26] M. Weinelt *et al.*, Phys. Rev. Lett. **92**, 126801 (2004).
[27] To estimate the energy barriers, the energy difference (per dimer) between the symmetric [parallel dimer, $p(2 \times 1)$ configuration (highest energy)] and the asymmetric $p(2 \times 1)$ is taken to be 120 meV. 100 meV is added to account for the 50 meV exchange energy with each nearest neighbor [K. Inoue *et al.*, Phys. Rev. B **49**, R14774 (1994)]. The value used for the local excitation is 11 meV [corresponding to an effective temperature on the order of 100 K, as in Ref. [17] ] at the position of the tip, with a decay length of 40 lattice units. The modeling will be discussed in more detail elsewhere [Y. Pennec *et al.* (to be published)].
[28] A. J. Heinrich *et al.*, Science **306**, 466 (2004).
[29] D. Atkinson *et al.*, Nat. Mater. **2**, 85 (2003).
[30] R. J. Hamers and U. K. Kohler, J. Vac. Sci. Technol. A **7**, 2854 (1989).